Published in final edited form as:
Nature. 2008 December 18; 456(7224): 962–966. doi:10.1038/nature07409.

Generation of cell polarity in plants links endocytosis, auxin distribution and cell fate decisions

Pankaj Dhonukshe[1], **Hirokazu Tanaka**[2,*], **Tatsuaki Goh**[3,*], **Kazuo Ebine**[3,*], **Ari Pekka Mähönen**[1,*], **Kalika Prasad**[1], **Ikram Blilou**[1], **Niko Geldner**[4,5], **Jian Xu**[1], **Tomohiro Uemura**[3], **Joanne Chory**[5], **Takashi Ueda**[3], **Akihiko Nakano**[3,6], **Ben Scheres**[1], and **Jiří Friml**[2]

[1] *Department of Biology, Faculty of Science, Utrecht University, Padualaan 8, 3584 CH, Utrecht, The Netherlands* [2] *Department of Plant Systems Biology, VIB, and Department of Molecular Genetics, Ghent University, Technologiepark 927, 9052 Gent, Belgium* [3] *Department of Biological Sciences, Graduate School of Science, University of Tokyo, Bunkyo-ku, Tokyo 113-0033, Japan* [4] *Department of Plant Molecular Biology (DBMV), University of Lausanne, UNIL-Sorge, Biophore Building, 1015 Lausanne, Switzerland* [5] *Plant Biology Laboratory, The Salk Institute for Biological Studies, La Jolla, California 92037, USA* [6] *Molecular Membrane Biology Laboratory, RIKEN Advanced Science Institute, Wako, Saitama 351-0198, Japan*

Abstract

Dynamically polarized membrane proteins define different cell boundaries and have an important role in intercellular communication—a vital feature of multicellular development. Efflux carriers for the signalling molecule auxin from the PIN family[1] are landmarks of cell polarity in plants and have a crucial involvement in auxin distribution-dependent development including embryo patterning, organogenesis and tropisms[2–7]. Polar PIN localization determines the direction of intercellular auxin flow[8], yet the mechanisms generating PIN polarity remain unclear. Here we identify an endocytosis-dependent mechanism of PIN polarity generation and analyse its developmental implications. Real-time PIN tracking showed that after synthesis, PINs are initially delivered to the plasma membrane in a non-polar manner and their polarity is established by subsequent endocytic recycling. Interference with PIN endocytosis either by auxin or by manipulation of the *Arabidopsis* Rab5 GTPase pathway prevents PIN polarization. Failure of PIN polarization transiently alters asymmetric auxin distribution during embryogenesis and increases the local auxin response in apical embryo regions. This results in ectopic expression of auxin pathway-associated root-forming master regulators in embryonic leaves and promotes homeotic transformation of leaves to roots. Our results indicate a two-step mechanism for the generation of PIN polar localization and the essential role of endocytosis in this process. It also highlights the link between endocytosis-dependent polarity of individual cells and auxin distribution-dependent cell fate establishment for multicellular patterning.

The plant signalling molecule auxin acts as a versatile trigger in many aspects of plant development and mediates different cellular responses on the basis of its graded distribution between cells. Establishment and maintenance of these auxin gradients requires local auxin biosynthesis[9,10] and directional cell-to-cell transport that depends on PIN auxin transporters[11]. PINs have a polar plasma membrane localization that determines the direction of intercellular auxin flow[8]. Thus, the mechanisms underlying PIN polarity belong to central

Correspondence and requests for materials should be addressed to P.D. (E-mail: P.B.Dhonukshe@uu.nl) or J.F. (E-mail: jiri.friml@psb.ugent.be).

*These authors contributed equally to this work.

Supplementary Information is linked to the online version of the paper at www.nature.com/nature.

aspects of auxin-mediated plant development. Polar PIN localization is dynamic; PIN proteins constitutively undergo cycles of clathrin-dependent endocytosis[12] and ARF-GEF-(guanine-nucleotide exchange factors for ADP-ribosylation factor GTPases)-dependent recycling[13]. The role of this constitutive cycling is unclear but it might account for rapid changes in PIN polarity[14] in response to different cues such as gravity[15]. Also, PIN phosphorylation controlled by PINOID kinase/PP2A phosphatase[16,17] and membrane sterol composition[18] are important components of polar PIN localization. However, it remains unresolved how PIN polarity is initially generated. In mammalian epithelia, segregation of membrane proteins into apical and basolateral plasma membrane domains is mainly achieved by polar exocytosis of newly synthesized proteins, or by non-polar exocytosis followed by endocytosis and polarized recycling[19]. Here we demonstrate an endocytosis-dependent mechanism for PIN polarity generation, and its importance for plant development.

To test the initial delivery of PINs to the plasma membrane, we photobleached pre-existing yellow fluorescent protein (YFP)-tagged PIN1 from a group of cells and analysed its recovery at the plasma membrane by *de novo* synthesis. This fluorescence recovery after photobleaching (FRAP) experiment showed an initial non-polar PIN1 localization followed by a gradual polarization of PIN1–YFP to the lower cell side (Fig. 1a, b). Using a complementary approach, we followed localization after conditional ectopic expression of PIN1. In inducible *XVE-PIN1* transgenic lines[1] 1 h after induction, PIN1 localizes strongly to intracellular compartments (presumably Golgi) and faintly throughout the plasma membrane in a non-polar manner. Over time, the intracellular PIN1 pool is reduced and non-polar PIN1 localization at the plasma membrane becomes stronger. About 3 h after induction PIN1 polarity is established showing predominant localization at the lower (basal) cell side (Fig. 1c). These observations suggest that, after *de novo* synthesis, PINs get targeted to the plasma membrane initially in a non-polar fashion and PIN polarity is generated in the subsequent step.

Next we tested the contribution of lateral diffusion within the plasma membrane for PIN polarity attainment. Locally photoconverted PIN2-EosFP displays limited lateral diffusion as compared to another plasma membrane-resident protein PIP2-EosFP, which shows much higher lateral diffusion (Supplementary Fig. 1). This suggests that lateral diffusion does not contribute considerably to asymmetric distribution of PINs at the plasma membrane. Therefore, we addressed the possibility that PIN polarity is generated from the original non-polar state by endocytic recycling (Fig. 1d). In this model, the inhibition of PIN endocytosis should interfere with PIN polarity generation. Auxin inhibits PIN internalization[20] and, accordingly, auxin treatment delays PIN1–YFP polarization after photobleaching (compare Fig. 1a, b and Supplementary Fig. 2a, b). Furthermore, endogenous or exogenously manipulated increases in cellular auxin levels correlate with decreased PIN polarity in corresponding cells (see Supplementary Information and Supplementary Fig. 2). These findings favour the hypothesis that after the original non-polar PIN targeting the polarity is generated by PIN internalization and subsequent recycling.

To investigate further the role of endocytosis in PIN polarity generation we sought to genetically interfere with endocytosis, allowing us to examine the so far elusive developmental role of this process in plants. An intensively studied Rab5 GTPase pathway has been shown to have a pivotal role for endocytosis in mammalian cells[21]. As two Rab5 homologues (namely Ara7 and Rha1) have been identified in *Arabidopsis* and localize to endosomes[22], we characterized single and double *ara7* and *rha1* mutants, as well as mutants for their common activator Rab5-GEF AtVps9a. *ara7* and *rha1* do not have noticeable phenotypic defects, whereas the *ara7 rha1* double mutant is gametophytic lethal (data not shown). In addition, the full knockout of *AtVps9a* (*atvps9a-1*) is embryonic lethal and the partial loss-of-function allele (*atvps9a-2*) is viable and shows phenotypic aberrations (see Supplementary Information and Supplementary Fig. 3). We also used another strategy by exploiting *Arabidopsis* lines

expressing a dominant negative Rab5 version (*DN-Ara7*) in which Rab5 is locked in its inactive state. Interference with the Rab5 pathway in *Arabidopsis* inhibited endocytosis (as monitored by an uptake of the fluorescent lipophylic dye FM4-64) without comparably influencing recycling or structure-dynamics of various subcellular compartments (see Supplementary Information and Supplementary Figs 4–7). Thus, the manipulation of the *Arabidopsis* Rab5 pathway provides a tool for investigating the role of endocytosis for diverse cellular and developmental processes in plants including its function in PIN polarity generation.

In *Arabidopsis* roots, PIN1 is localized preferentially at the basal (root tip-facing) side of stele cells[23] (Fig. 2a) and PIN2 is at the apical (shoot tip-facing) side of epidermis cells (Fig. 2b) and located basally in young cortex cells (Fig. 2b)[24]. In *atvps9a-2* mutants, or after short-term (4 h) induction of *DN-Ara7* expression, PIN1 and PIN2 show less polar plasma membrane distribution (Fig. 2a–d). The effect of *DN-Ara7* on polar PIN2 localization is more pronounced in the cortex than in the epidermis (Fig. 2b; see also the insets for cortical PIN2 localization). After the ectopic expression of PIN1 in *XVE-PIN1* lines, freshly synthesized PIN1 arrives at the plasma membrane in a non-polar manner, in wild type (Fig. 1c) as well as after pre- and co-induction of *DN-Ara7* expression (Fig. 2e). However, whereas PIN1 subsequently polarizes in the wild type (Fig. 1c and 2e) it sustains its initial non-polar localization in *DN-Ara7* (Fig. 2e). Taking into account the fact that interference with the Rab5 pathway does not visibly influence PIN secretion or recycling, we conclude that Rab5-mediated endocytosis is required for acquisition of PIN polar localization. Furthermore, the mostly unaltered polar localization of another polar marker auxin influx carrier AUX1 (ref. 25) in *DN-Ara7* (Supplementary Fig. 8) suggests that there is a certain specificity of the Rab5-dependent endocytic mechanism for PIN polarization. This is consistent with previous findings that PIN and AUX1 use distinct polarity pathways[26].

Next we assessed the developmental importance of Rab5-mediated endocytosis by analysing PIN polarity, auxin distribution and development in *DN-Ara7* and *atvps9a-1* embryos. In embryos expressing *DN-Ara7* under the control of a strong embryonic RPS5A promoter[27] and in *atvps9a-1* embryos PIN1 (Fig. 3a) and PIN4 (data not shown) lose their basal polar localization, resulting in a largely non-polar distribution. Because patterning during embryogenesis requires PIN-dependent asymmetric auxin distribution (auxin gradients)[3], we next tested the consequences of PIN polarity defects for spatial distribution of auxin activity and for embryonic patterning. In controls, auxin activity as monitored by the auxin responsive reporter *DR5* shows its normal pattern[3] with strong maxima at the root pole and weaker maxima at the cotyledon tips (Fig. 3b). In contrast, in *atvps9a-1* (data not shown) or *RPS5A≫DN-Ara7* (Fig. 3b) embryos, the *DR5* maxima are less clearly defined with ectopically increased DR5 activity in developing cotyledons. Analysis of embryo development showed that control embryos have typical developmental stage-specific phenotypes, whereas in *RPS5A≫DN-Ara7* embryos phenotypic abnormalities occur from octant stage onwards and they become more pertinent from the globular stage onwards (Fig. 3c and Supplementary Fig. 9). Typically, cell division planes are altered at the root pole, the cotyledons are occasionally fused and a new outgrowing structure appears in the apical region (Fig. 3c and Supplementary Fig. 9). Similar although less pronounced defects are also observed in *atvps9a-1* embryos (data not shown). These results indicate that the failure of PIN polarization, resulting from the inhibition of Rab5-mediated endocytosis, leads to perturbation in asymmetric auxin distribution and embryo development.

We next analysed the postembryonic consequences of interference with the Rab5-mediated endocytosis. As the full *atvps9a* knockout is embryo lethal, we analysed the postembryonic development in *RPS5A≫DN-Ara7* seedlings. In parallel, to bypass the early embryonic development, we created RNA interference (RNAi)-based *AtVps9a* silencing lines under the control of the CaMV35S promoter (Supplementary Fig. 12), which is only weakly active in

early embryogenesis[28]. *RPS5A≫DN-Ara7* seedlings remain small compared to controls and show pronounced root and cotyledon defects (Fig. 4a). Notably, in approximately 15% of the seedlings (31 out of 200), cotyledons develop new, chlorophyll-free structures at their tips (see inset in Fig. 4a and Supplementary Fig. 10). Morphologically these structures clearly differ from occasional cases of necrotic tissue and mostly resemble young root primordia. In rare cases these root-like structures emerging from the cotyledon tips develop further to form normally appearing growing roots (Fig. 4b). Similar although less frequent (17 out of 165 T_1 plants) developmental aberrations, including the ectopic appearance of root-like structures, were observed in *AtVps9a*(*RNAi*) (inset in Fig. 4a and Supplementary Fig. 12). In later development of both *RPS5A≫DN-Ara7* and *AtVps9a*(*RNAi*) seedlings, the cotyledon-derived, root-like structures terminally differentiate and these seedlings are not viable (data not shown).

To examine further the identity of the root-like structures, we analysed cell morphologies at scanning electron microscopy (SEM) resolution. Control cotyledons and hypocotyls show cells interspersed with stomata (Fig. 4c, d and Supplementary Fig. 10). In contrast, the root-like structures have distinct narrower rectangular epidermal cells devoid of stomata resembling root epidermis (Fig. 4d). In addition, transformed and growing root-like structures develop root hairs similar to the main root (Fig. 4b). Notably, molecular identity markers confirm the root identity of the root-like structures. We detected ectopic expression of root-specific quiescent cell marker QC25 (ref. 23) at the tips of *RPS5A≫DN-Ara7* cotyledons and also in seedlings that do not show morphologically distinguishable root-like structures (Supplementary Fig. 11). Furthermore, root-like structures in *AtVps9a*(*RNAi*) seedlings express the root-specific PIN2 protein[7] (Supplementary Fig. 12). Thus, both morphological and molecular markers confirm homeotic transformation of leaves to roots in seedlings perturbed for the Rab5 pathway.

Next we addressed the mechanism by which inhibition of the Rab5-dependent pathway can lead to transformation of organ identities. As the formation of root-like structures spatially coincides with elevated auxin response at cotyledons during embryogenesis, the most straightforward explanation is that this increased auxin response triggers a root-specific developmental programme. An obvious candidate for a mediator of such a change is one of the auxin response-dependent master regulators of root formation, the transcription factor PLT1 (ref. 29). Indeed, we detected strong, ectopic expression of PLT1 in postglobular *RPS5A≫DN-Ara7* embryos at positions of auxin maxima (Fig. 4e). The ectopic expression of other markers, such as root cap-specific PIN3 (ref. 15) and a root quiescent centre-specific WOX5 (ref. 30), is also detected at these positions in addition to their normal expression at the root pole (Fig. 4e). These data show that in *RPS5A≫DN-Ara7* and in *AtVps9a*(*RNAi*) lines cotyledon identity changes to root identity at positions of increased auxin response maxima during embryogenesis. It seems that timing is particularly important in this case. Although embryonic cells are still competent for such marked alterations in developmental programs, when we impaired the Rab5 pathway during post-germination development (in tamoxifen-inducible *DN-Ara7* lines) we failed to observe any organ identity aberrations although we did detect defects in other auxin-related processes such as root gravitropism and lateral root formation (Supplementary Fig. 13).

A plausible mechanism underlying the observed homeotic organ transformations is that defects in endocytosis cause failure of PIN polarization leading to ectopic auxin accumulation at the place of auxin synthesis in the cotyledons[9,10], in which downstream PLT expression ultimately leads to transformation of cotyledon fates into root fates. It is surprising, however, that interference with Rab5-dependent endocytosis, which affects several plasma membrane-localized proteins (Supplementary Fig. 4), would show apparently specific auxin-related patterning defects. To more directly address the link between PIN polarity, auxin distribution and organ identity, we used *RPS5A::PIN1-GFP2* that shows strong expression and largely non-polar localization of PIN1–GFP2 in embryos (Supplementary Fig. 14). In wild-type

RPS5A::PIN1-GFP2 seedlings, the cotyledon-originated root-like structure phenotype was observed at lower frequency (4 out of 129 in the T_2 generation). However, in multiple *pin* mutant background (*pin* $1^{+/-}2347^{+/-}$), with limited extent of endogenous polarized PINs, this homeotic transformation was already detected in the T_1 generation at markedly increased frequency (23 out of 26; Supplementary Fig. 14). Furthermore, as observed in *RPS5A≫DN-Ara7* embryos (Fig. 3b), *RPS5A::PIN1-GFP2* embryos showed increased auxin response at cotyledon regions apparently marking the positions of later-emerging root structures (Supplementary Fig. 14). These results strongly indicate that the homeotic leaf-to-root transformation in Rab5-defective plants can be largely attributed to the failure of PIN polarization and to the resulting changes in auxin distribution. Our data further highlight the important role of endocytosis in PIN polarization and its connection to auxin-dependent establishment of cell fates for plant patterning.

Our studies suggest an endocytosis-dependent, two-step mechanism for PIN polarity generation. We show that PINs are first targeted to the plasma membrane without apparent asymmetry, and they then attain polarity by subsequent endocytic recycling. The endocytic step is crucial for the polarity establishment because interference with PIN internalization, for example by increasing auxin amounts or interfering with the Rab5-based endocytic pathway, sustains initial non-polar PIN localization leading to polarity defects. The failure of PIN polarization during embryogenesis apparently disrupts auxin flow from developing cotyledons to the root pole, and consequently auxin levels here increase from auxin production, leading to the establishment of ectopic auxin response maxima at cotyledon positions. Embryonic cells are competent at this stage to interpret the increased auxin response as a positional signal for root formation and accordingly they express the root fate-promoting transcription factor PLT1 that sets up the initiation of roots at the positions of embryonic leaves (Fig. 4f). These results demonstrate important cellular and developmental roles for endocytosis in plants and highlight the morphogenetic features of transport-dependent auxin distribution in plant patterning processes.

METHODS SUMMARY

Materials and growth conditions

Arabidopsis seedlings (Columbia ecotype) were grown on vertical 0.5 MS agar plates at 25 ° C. FM4-64, BFA (both Molecular Probes), tamoxifen and estradiol (both Sigma) were used from dimethylsulphoxide stock solutions (1 mM for FM4-64, 50 mM for BFA, 3 mM for tamoxifen and 1 mM for estradiol) and added (at 1:1,000 dilution) either to the liquid 0.5 MS growth medium or to the 0.5 MS growth medium plates for the indicated periods of time.

Immunodetection

Immunofluorescence analysis in *Arabidopsis* roots was carried out as described previously[12].

Embryo and *in situ* analysis

Embryo and *in situ* analysis was performed as described previously[3,24].

Microscopy

For SEM, seedlings were fixed, dehydrated and then critical point dried. The dried seedlings were mounted onto stubs, sputter coated with platinum and then viewed in a Joel JSM-5310 LV microscope. Live cell microscopy, FRAP analysis and EosFP green-to-red photoconversion analysis were performed as described previously[12].

METHODS

Cloning details and *Arabidopsis* transgenic lines

A 6.1 kb genomic fragment of *AtVps9a* containing promoter, exons, introns and the 3′-flanking region was fused to *GFP* to have a carboxy-terminal *GFP*-fusion which was used for complementation and localization analyses. The complemented line was again transformed with *mRFP-ARA7* and used for colocalization analysis. Construction of *DN-Ara7* by site-directed mutagenesis of wild-type Ara7 (by replacing S24N) has been described before[31]. For transactivation approach *DN-Ara7* was cloned under the *UAS* promoter and transferred to binary vector *pGreenII* that was used for transformation. The *AtVps9a*(*RNAi*) construct was obtained from the NASC *Arabidopsis* stock centre. *GFP* complementary DNA was fused to the genomic fragment of *SYP43* containing promoter (2,039 base pairs (bp)), exons, introns and the 3′-flanking region (782 bp) to have an amino-terminal *GFP*-fusion. This chimaeric construct was transformed into the *syp43* mutant line in which the T-DNA is inserted at the second intron and also in *atvps9a-2*. For cloning *RPS5A::PIN1-GFP2*, the *RPS5A* promoter was amplified from a recombinant construct *pGII/K RPS5A t-NOS*[27] and *PIN1-GFP2* was amplified from a *pG2NBL-PIN1::PIN-EGFP* plasmid[32]. *RPS5A::PIN1-GFP2* was then introduced into *pGreenII* binary vector using Multisite Gateway technology (Invitrogen). The root cap-specific *PIN2-EGFP* line was generated from *PIN2::PIN2-EGFP*[33], by cloning the *PIN2-EGFP* fusion (from ATG to the stop codon) into *pGREENII-0229* between a 3.3 kilobase (kb) promoter fragment of the *At1g79580* gene and the *NOS* terminator. Construction of PIP2-EosFP has been described earlier[12].

The following mutant and transgenic *Arabidopsis* lines have been described previously: *PIN1-YFP*[32], *PIN2-GFP*[32], *RPS5A* activator[27], *pINTAM* activator[16], *XVE-PIN1* (ref. 1), *PIN2-EosFP*[12], *DR5rev::ER-GFP*[3], *DR5rev::3×VENUS-N7* (ref. 6), *VPS29-RFP*[34], *SNX1-RFP*[34], *GNOM-Myc*[35], *GNL1-YFP*[36], *VHAa1-RFP*[37], *AUX1-YFP*[38], *QC25-GUS*[39] and *pin*$^{+/-}$*12347*$^{+/-}$ (ref. 24). Isolation and the initial characterization of *atvps9a* mutants is described elsewhere[40]. *ara7* (WiscDsLox355B06), *rha1* (SAIL_596-A03) and *syp43* (SALK_144268) are obtained from the ABRC.

Construction of fusion proteins and *Arabidopsis* transgenic lines for *NPSN12-YFP*, *PIP1-YFP*, *NIP1-YFP*, *RabA5d-YFP*, *SYP32-YFP*, *RabD2B-YFP*, *RabG3f-YFP* and *VAMP711-YFP* will be described elsewhere (N.G. and J.C., unpublished observations). Information on these lines is available at http://www.unil.ch/dbmv/page49637_en.html. These lines were crossed with *pINTAM≫DN-Ara7* line for analysing effect of DN-Ara7 on localization and BFA sensitivity of these markers. Sequences of the primers used are mentioned in Supplementary Table 1.

Immunodetection

The following antibodies were used: anti-PIN1 (1:400)[3], anti-PIN2 (1:1,000)[41], anti-PIN4 (1:400)[23], anti-SCAMP1 (1:200)[42], anti-plasma-membrane-ATPase (1:1,000)[43], anti-γ-COP (1:1,000)[44] and anti-GFP (1:400). Fluorochrome-conjugated secondary antibodies (Dianova) were used at the following concentrations: anti rabbit-FITC (1:300); anti-rabbit-Cy3 (1:500) and anti-mouse-FITC (1:300). The same microscope settings were used for different experiments and pixel intensities were taken into account when comparing the images. All experiments were performed at least three times using at least 20 roots on each occasion.

Quantification of PIN polarity

The mean fluorescence intensity of the PIN signal at the lateral and polar sides of cells was measured using the quantification tool of Leica confocal software (LCS Lite Version 2.61). This tool provides the opportunity to draw lines on the lateral or polar cell side. It also enables

the value of mean pixel intensity of the area covered by the drawn line to be obtained. Using this procedure, the mean pixel intensities from the polar and lateral cell sides of individual cells were obtained. They were then used to determine the polarity index—the ratio of PIN intensity at polar versus lateral sides. The mean and s.d. of the polarity index were determined for the number of samples analysed for the condition tested.

Supplementary Material

Refer to Web version on PubMed Central for supplementary material.

Acknowledgments

We thank M. Bennett, T. Gaude, L. Jiang, G. Jürgens, C. Luschnig, E. Meywerowitz, W. Michalke, R. Offringa, D. Robinson, K. Schumacher, J. Wiedenmann and D. Weijers for sharing published material and RIKEN, SALK and NASC *Arabidopsis* stock centres for providing mutant lines and the RNAi construct. We thank W. Muller for assistance with SEM and F. Kindt and R. Leito for photography. We acknowledge the Center for Plant Molecular Biology (ZMBP), University of Tübingen, Germany for the facilities during the initial phase of the project. This work was supported by VolkswagenStiftung (P.D. and J.F.), EMBO Long Term Fellowship and Netherlands Organization for Scientific Research (NWO)-VENI grant (P.D.), EMBO Young Investigator Program and Odysseus program of FWO (J.F.), HFSP fellowship (H.T.), EMBO Long Term Fellowship and HFSP fellowship (A.P.M.), EMBO Long Term Fellowship (K.P.), NWO-VIDI grant (I.B.), HFSP fellowship and Swiss National Science Foundation (N.G.), HHMI, USDA and NIH (J.C.), NWO-Spinoza award (B.S.) and Grants-in-Aid for Scientific Research from the Ministry of Education, Culture, Sports, Science and Technology of Japan (T.U. and A.N.).

References

1. Petrasek J, et al. PIN proteins perform a rate-limiting function in cellular auxin efflux. Science 2006;312:914–918. [PubMed: 16601150]
2. Galweiler L, et al. Regulation of polar auxin transport by AtPIN1 in *Arabidopsis* vascular tissue. Science 1998;282:2226–2230. [PubMed: 9856939]
3. Friml J, et al. Efflux-dependent auxin gradients establish the apical-basal axis of *Arabidopsis*. Nature 2003;426:147–153. [PubMed: 14614497]
4. Benkova E, et al. Local, efflux-dependent auxin gradients as a common module for plant organ formation. Cell 2003;115:591–602. [PubMed: 14651850]
5. Reinhardt D, et al. Regulation of phyllotaxis by polar auxin transport. Nature 2003;426:255–260. [PubMed: 14628043]
6. Heisler MG, et al. Patterns of auxin transport and gene expression during primordium development revealed by live imaging of the *Arabidopsis* inflorescence meristem. Curr Biol 2005;15:1899–1911. [PubMed: 16271866]
7. Luschnig C, Gaxiola RA, Grisafi P, Fink GR. EIR1, a root-specific protein involved in auxin transport, is required for gravitropism in *Arabidopsis* thaliana. Genes Dev 1998;12:2175–2187. [PubMed: 9679062]
8. Wisniewska J, et al. Polar PIN localization directs auxin flow in plants. Science 2006;312:883. [PubMed: 16601151]
9. Stepanova AN, et al. TAA1-mediated auxin biosynthesis is essential for hormone crosstalk and plant development. Cell 2008;133:177–191. [PubMed: 18394997]
10. Zhao Y. The role of local biosynthesis of auxin and cytokinin in plant development. Curr Opin Plant Biol 2008;11:16–22. [PubMed: 18409210]
11. Tanaka H, Dhonukshe P, Brewer PB, Friml J. Spatiotemporal asymmetric auxin distribution: a means to coordinate plant development. Cell Mol Life Sci 2006;63:2738–2754. [PubMed: 17013565]
12. Dhonukshe P, et al. Clathrin-mediated constitutive endocytosis of PIN auxin efflux carriers in *Arabidopsis*. Curr Biol 2007;17:520–527. [PubMed: 17306539]
13. Geldner N, Friml J, Stierhof YD, Jurgens G, Palme K. Auxin transport inhibitors block PIN1 cycling and vesicle trafficking. Nature 2001;413:425–428. [PubMed: 11574889]

14. Kleine-Vehn J, et al. ARF GEF-dependent transcytosis and polar delivery of PIN auxin carriers in *Arabidopsis*. Curr Biol 2008;18:526–531. [PubMed: 18394892]
15. Friml J, Wisniewska J, Benkova E, Mendgen K, Palme K. Lateral relocation of auxin efflux regulator PIN3 mediates tropism in *Arabidopsis*. Nature 2002;415:806–809. [PubMed: 11845211]
16. Friml J, et al. A PINOID-dependent binary switch in apical-basal PIN polar targeting directs auxin efflux. Science 2004;306:862–865. [PubMed: 15514156]
17. Michniewicz M, et al. Antagonistic regulation of PIN phosphorylation by PP2A and PINOID directs auxin flux. Cell 2007;130:1044–1056. [PubMed: 17889649]
18. Men S, et al. Sterol-dependent endocytosis mediates post-cytokinetic acquisition of PIN2 auxin efflux carrier polarity. Nature Cell Biol 2008;10:237–244. [PubMed: 18223643]
19. Mostov K, Su T, ter Beest M. Polarized epithelial membrane traffic: conservation and plasticity. Nature Cell Biol 2003;5:287–293. [PubMed: 12669082]
20. Paciorek T, et al. Auxin inhibits endocytosis and promotes its own efflux from cells. Nature 2005;435:1251–1256. [PubMed: 15988527]
21. Bucci C, et al. The small GTPase rab5 functions as a regulatory factor in the early endocytic pathway. Cell 1992;70:715–728. [PubMed: 1516130]
22. Ueda T, Uemura T, Sato MH, Nakano A. Functional differentiation of endosomes in *Arabidopsis* cells. Plant J 2004;40:783–789. [PubMed: 15546360]
23. Friml J, et al. AtPIN4 mediates sink-driven auxin gradients and root patterning in *Arabidopsis*. Cell 2002;108:661–673. [PubMed: 11893337]
24. Blilou I, et al. The PIN auxin efflux facilitator network controls growth and patterning in *Arabidopsis* roots. Nature 2005;433:39–44. [PubMed: 15635403]
25. Swarup R, et al. Localization of the auxin permease AUX1 suggests two functionally distinct hormone transport pathways operate in the *Arabidopsis* root apex. Genes Dev 2001;15:2648–2653. [PubMed: 11641271]
26. Kleine-Vehn J, Dhonukshe P, Swarup R, Bennett M, Friml J. Subcellular trafficking of the *Arabidopsis* auxin influx carrier AUX1 uses a novel pathway distinct from PIN1. Plant Cell 2006;18:3171–3181. [PubMed: 17114355]
27. Weijers D, et al. An *Arabidopsis* Minute-like phenotype caused by a semi-dominant mutation in a *RIBOSOMAL PROTEIN S5* gene. Development 2001;128:4289–4299. [PubMed: 11684664]
28. Benfey PN, Chua NH. The cauliflower mosaic virus 35S promoter: combinatorial regulation of transcription in plants. Science 1990;250:959–966. [PubMed: 17746920]
29. Aida M, et al. The PLETHORA genes mediate patterning of the *Arabidopsis* root stem cell niche. Cell 2004;119:109–120. [PubMed: 15454085]
30. Sarkar AK, et al. Conserved factors regulate signalling in *Arabidopsis* thaliana shoot and root stem cell organizers. Nature 2007;446:811–814. [PubMed: 17429400]
31. Dhonukshe P, et al. Endocytosis of cell surface material mediates cell plate formation during plant cytokinesis. Dev Cell 2006;10:137–150. [PubMed: 16399085]
32. Xu J, et al. A molecular framework for plant regeneration. Science 2006;311:385–388. [PubMed: 16424342]
33. Xu J, Scheres B. Dissection of *Arabidopsis* ADP-RIBOSYLATION FACTOR 1 function in epidermal cell polarity. Plant Cell 2005;17:525–536. [PubMed: 15659621]
34. Jaillais Y, et al. The retromer protein VPS29 links cell polarity and organ initiation in plants. Cell 2007;130:1057–1070. [PubMed: 17889650]
35. Geldner N, et al. The *Arabidopsis* GNOM ARF-GEF mediates endosomal recycling, auxin transport, and auxin-dependent plant growth. Cell 2003;112:219–230. [PubMed: 12553910]
36. Richter S, et al. Functional diversification of closely related ARF-GEFs in protein secretion and recycling. Nature 2007;448:488–492. [PubMed: 17653190]
37. Dettmer J, Hong-Hermesdorf A, Stierhof YD, Schumacher K. Vacuolar H^+-ATPase activity is required for endocytic and secretory trafficking in *Arabidopsis*. Plant Cell 2006;18:715–730. [PubMed: 16461582]
38. Swarup R, et al. Structure-function analysis of the presumptive *Arabidopsis* auxin permease AUX1. Plant Cell 2004;16:3069–3083. [PubMed: 15486104]

39. Sabatini S, et al. An auxin-dependent distal organizer of pattern and polarity in the *Arabidopsis* root. Cell 1999;99:463–472. [PubMed: 10589675]

40. Goh T, et al. VPS9a, the common activator for two distinct types of Rab5 GTPases, is essential for the development of *Arabidopsis* thaliana. Plant Cell 2007;19:3504–3515. [PubMed: 18055610]

41. Abas L, et al. Intracellular trafficking and proteolysis of the *Arabidopsis* auxin-efflux facilitator PIN2 are involved in root gravitropism. Nature Cell Biol 2006;8:249–256. [PubMed: 16489343]

42. Lam SK, et al. Rice SCAMP1 defines clathrin-coated, *trans*-golgi-located tubular-vesicular structures as an early endosome in tobacco BY-2 cells. Plant Cell 2007;19:296–319. [PubMed: 17209124]

43. Langhans M, et al. Immunolocalization of plasma-membrane H^+-ATPase and tonoplast-type pyrophosphatase in the plasma membrane of the sieve element-companion cell complex in the stem of *Ricinus communis* L. Planta 2001;213:11–19. [PubMed: 11523647]

44. Movafeghi A, Happel N, Pimpl P, Tai GH, Robinson DG. *Arabidopsis* Sec21p and Sec23p homologs Probable coat proteins of plant COP-coated vesicles. Plant Physiol 1999;119:1437–1446. [PubMed: 10198103]

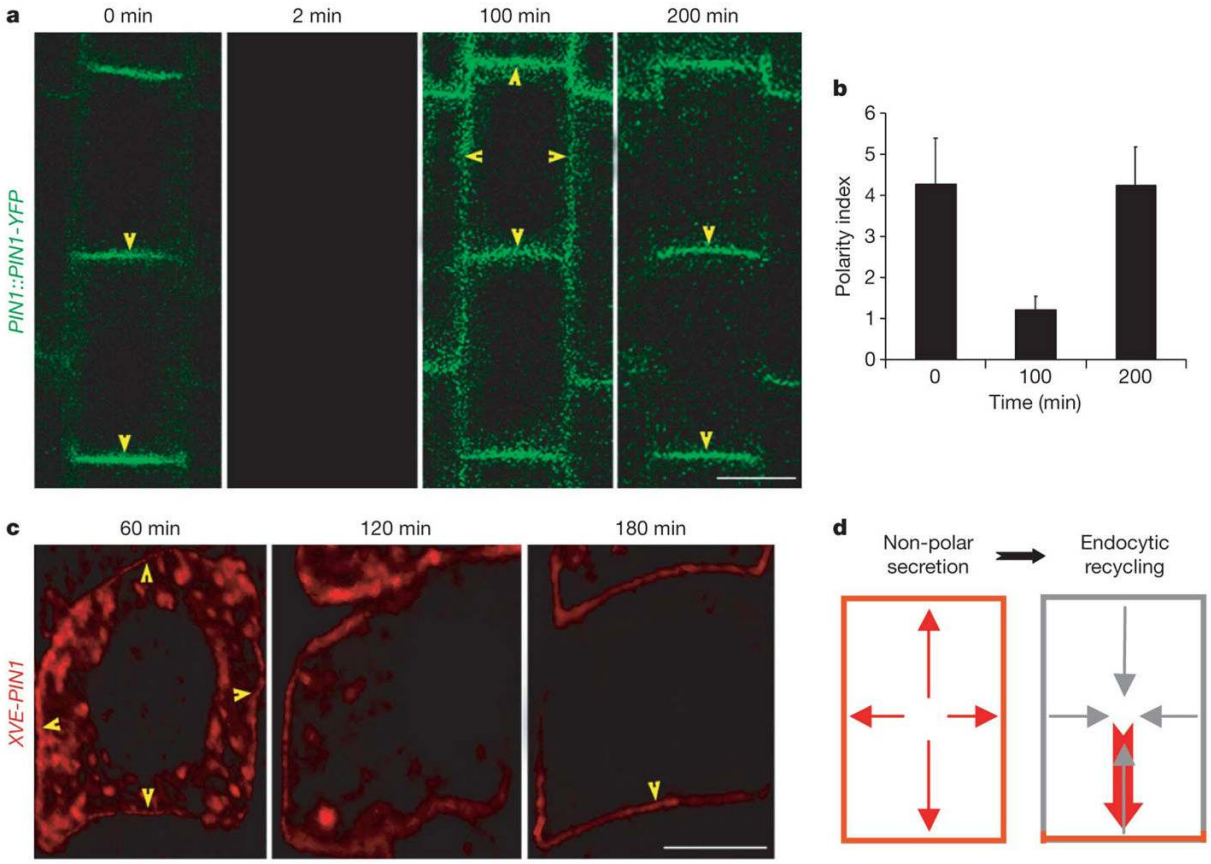

Figure 1. Endocytic recycling-based two-step mechanism generates PIN polarity

a, Targeting of newly synthesized PIN1–YFP to the plasma membrane after its complete photobleaching. Note PIN1–YFP localization (yellow arrowheads) at the plasma membrane in a non-polar manner (third panel) before becoming polar (fourth panel). **b**, Quantitative polarity index (ratio of polar to lateral PIN1–YFP intensity) for FRAP experiments. Data are mean and s.d.; $n = 15$. **c**, Inducible overexpression of PIN1 in *XVE-PIN1* epidermal cells shows PIN1 localization (yellow arrowheads) in the intracellular compartments and weak non-polar localization at the plasma membrane (first panel) after 1 h. At later time points, PIN1 shows gradually reduced intracellular signal and establishment of polar plasma membrane localization (third panel). **d**, A two-step mechanism for PIN polarity generation is shown. First, there is default non-polar secretion to the plasma membrane, followed by endocytic recycling establishing polarity. All are root cells. Scale bars are 5 μm.

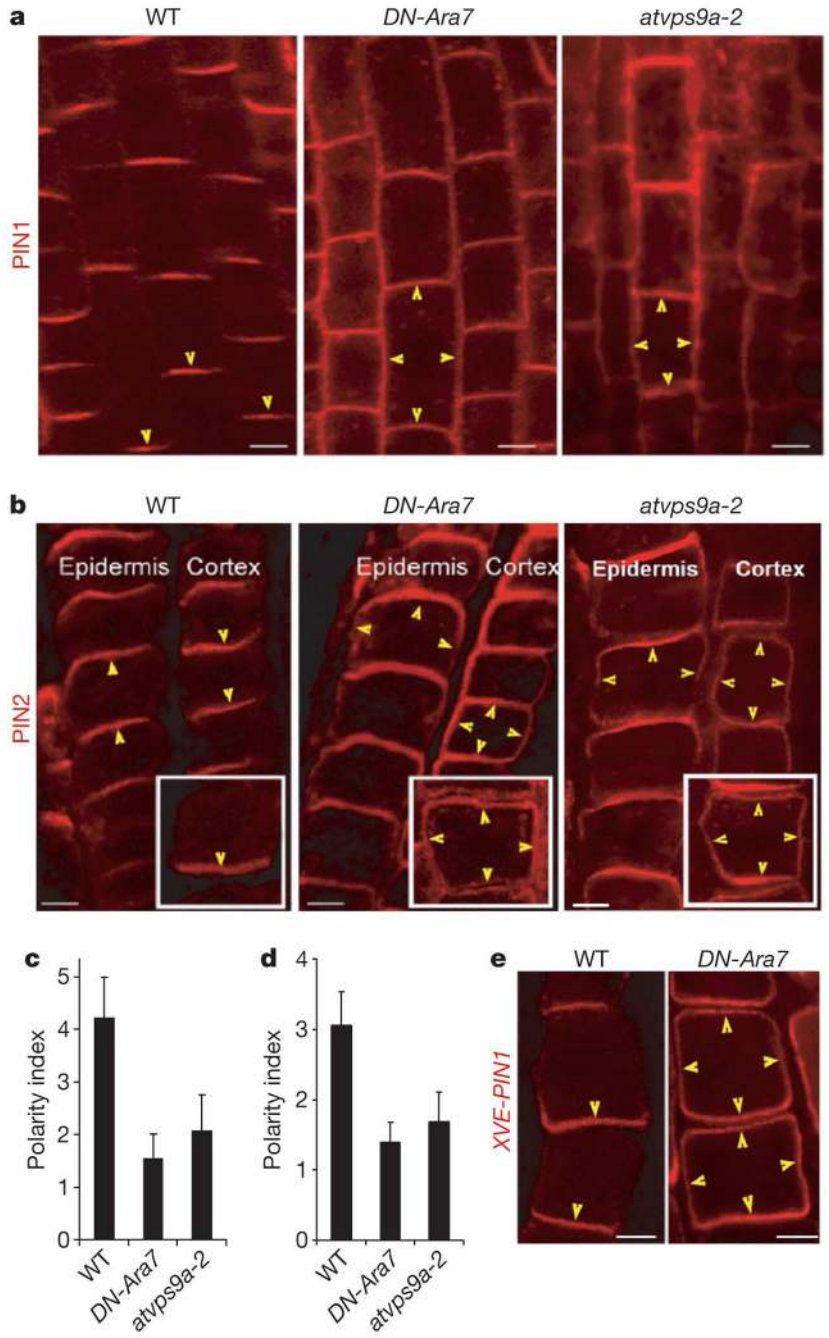

Figure 2. Rab5-mediated endocytosis is required for PIN polarization

a, **b**, PIN1 (**a**) and PIN2 (**b**) polarity is defective in *DN-Ara7* and *atvps9a-2*. Note the polar localization of PINs in wild type (WT; left panels, yellow arrowheads) and their largely non-polar localization in *DN-Ara7* and *atvps9a-2* (middle and right panels, yellow arrowheads). **c**, **d**, Quantitative evaluation of PIN1 (**c**) and PIN2 (**d**) polarity defects. Data are mean and s.d.; *n* =63 and 38 (**c** and **d**, respectively). **e**, Post-induction (3 h) *XVE-PIN1* localization in wild type and in *DN-Ara7*. Note that in wild type (WT) induced PIN1 becomes polar (left panel, yellow arrowheads), whereas in *DN-Ara7* seedlings it remains largely non-polar (right panel, yellow arrowheads). All are root cells. Scale bars are 5 μm.

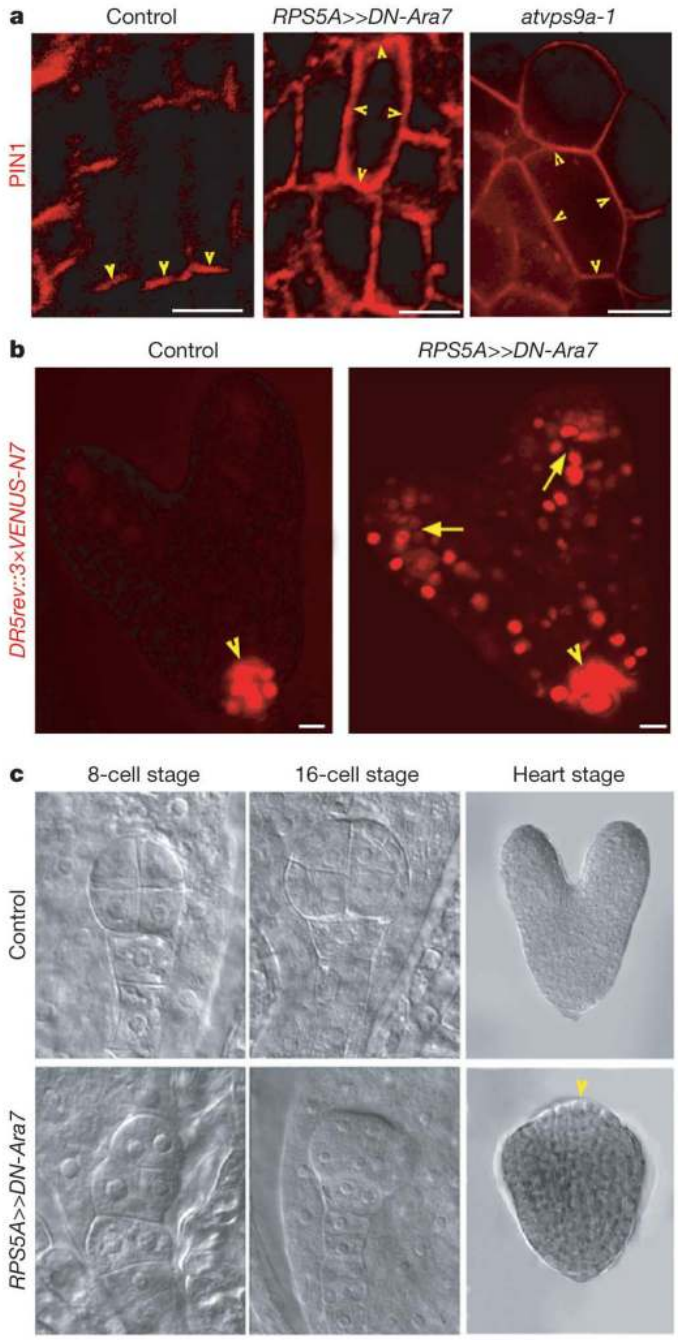

Figure 3. Manipulation of the Rab5 pathway during embryogenesis leads to defects in PIN polarity, auxin response distribution and embryo development

a, PIN1 polarity (yellow arrowheads) defects in the heart-shaped embryos in *RPS5A≫DN-Ara7* and in the embryo-lethal *atvps9a-1* mutant as compared to control. Note that PIN1 is localized basally in control (left) and is largely non-polar in both *RPS5A≫DN-Ara7* (middle) and *atvps9a-1* (right) mutants. **b**, Distribution of auxin response (visualized by *DR5rev::3×VENUS-N7*) is altered in the *RPS5A≫DN-Ara7* heart-shaped embryo. Note pronounced DR5 maxima at the root pole in control (left panel, yellow arrowhead) and *RPS5A≫DN-Ara7* embryos and further strong DR5 maxima in cotyledons (right panel, yellow arrows) of *RPS5A≫DN-Ara7* embryos. **c**, Embryonic defects from the 8-cell stage up to the heart-shaped

stage in *RPS5≫DN-Ara7* as compared to control. Note apical embryonic defects (bottom right, yellow arrowhead) in *RPS5≫DN-Ara7*. All are embryonic cells. Scale bars are 10 μm.

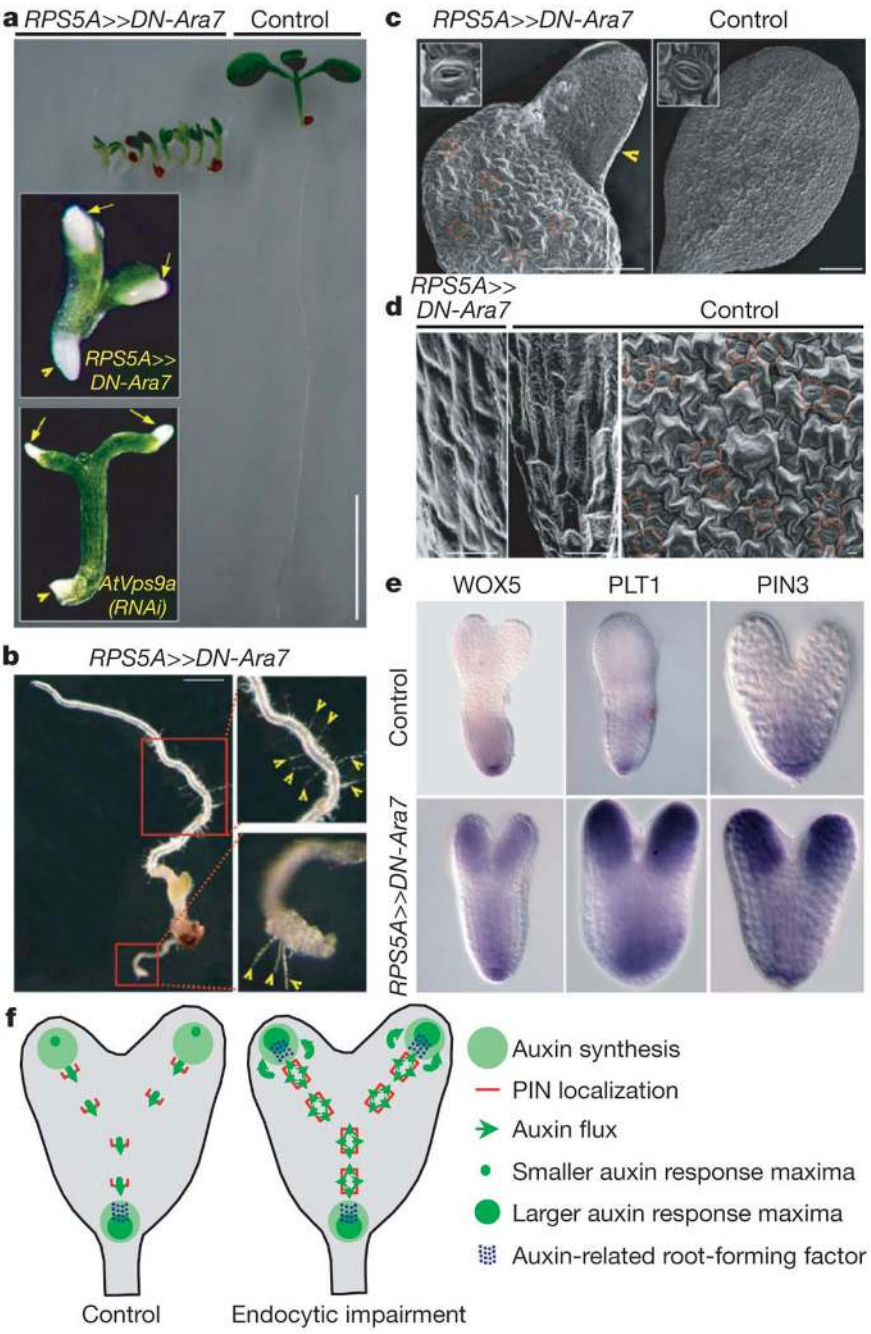

Figure 4. Manipulation of Rab5 pathway leads to homeotic leaf-to-root transformation

a, Phenotypic comparison of 6-day-old control and *RPS5A≫DN-Ara7* seedlings. Insets show root-like structures emerging from the embryonic leaves (cotyledons) in *RPS5A≫DN-Ara7* and in *35S::AtVps9a*(*RNAi*) seedlings. Yellow arrows represent the root-like structures emerging from the embryonic leaves, whereas yellow arrowheads represent the main root. **b**, Two separate growing roots in *RPS5A≫DN-Ara7* 3-week-old seedling. One root emerges from the root pole and another from the position of cotyledon. Note that both roots have root hairs (root-specific epidermal structures highlighted by yellow arrowheads). **c**, **d**, SEM analysis of *RPS5A≫DN-Ara7* and control. Stomata, a non-root cell type (red dotted circles, enlarged in

insets) are absent from the root-like structure (yellow arrowhead, **c**). Epidermal cells of root-like structure (left panel, **d**), with narrow rectangular cell files, are clearly distinct from cotyledon pavement cells of control (right panel, **d**) and resemble main root epidermal cells of control (middle panel, **d**). **e**, *In situ* hybridization reveals ectopic expression of the root-specific transcription factor PLT1 and the root meristem-identity markers WOX5 and PIN3 in cotyledons of *RPS5A≫DN-Ara7* heart-stage embryos. Note that expression of these markers is restricted to the root pole of control embryos. **f**, A schematic representation depicting enhanced auxin response maxima at the cotyledon regions resulted from non-polar PIN localization. This increased auxin response at the cotyledon regions leads to expression of auxin-induced root-forming regulators and triggers cell fate changes resulting in homeotic leaf-to-root transformation. Scale bars: 4 mm (**a**), 1 mm (**b**), 250 μm (**c**) and 10 μm (**d**).